

# Synthesis of C/ZnO/CdS nanocomposite with enhanced visible light photocatalytic activity

Yuvraj S. Malghe\*, Atul B. Lavand

Department of Chemistry, The Institute of Science, Mumbai 400032, India

\*Corresponding author. Tel: (+91) 22-22844219; Fax: (+91) 22-22816750; E-mail: ymalghe@yahoo.com

Received: 01 September 2015, Revised: 27 November 2015 and Accepted: 02 January 2016

## ABSTRACT

C/ZnO/CdS nanocomposite was synthesized using microemulsion method. Thermal stability of precursor was studied with TG and DTA techniques. Structural and optical properties of composite were studied using various characterization techniques like X-ray diffraction (XRD), fourier transform infrared spectroscopy (FTIR), field emission scanning electron microscopy (FESEM), energy dispersive x-ray spectroscopy (EDX), transmission electron microscopy (TEM) and UV-visible absorption spectroscopy and photoluminescence spectroscopy. XRD study indicates that ZnO and CdS are having wurtzite and cubic phase in the composite sample. SEM and TEM study indicates formation of CdS nanospheres on ZnO nanorods. C doping and CdS coupling are responsible for red shift and shifting of absorption edge of ZnO from UV to visible region. C/ZnO/CdS nanocomposite exhibits better visible light photocatalytic activity for degradation of methylene blue (MB). Stability of photocatalyst was studied using recovered photocatalyst up to third cycle and it was found that photocatalyst prepared in the present work is stable and reusable. Copyright © 2016 VBRI Press.

**Keywords:** Visible light; photocatalysis; ZnO; C doping; CdS.

## Introduction

Methylene blue (MB) is a heterocyclic aromatic chemical compound with a molecular formula  $C_{16}H_{18}N_3SCl$ . It has number of applications in various fields. It is used as a dye for a number of staining procedures such as Wright's stain, Jenner's stain etc. Since it is a temporary staining technique, MB is also used to examine RNA or DNA under the microscope or in a gel. It is also used as an indicator to determine if a cell such as yeast is alive or dead. Beside these numerous applications MB has lot of adverse reactions in environment and on human being such as hypertension, mental confusion, staining of skin, nausea, discoloration of urine, anaemia, precordial pain, headache, vomiting, bladder irritation, fever and abdominal pain. Dye pollutants from industries are important source of MB contamination. Large amount of unconsumed MB produced by chemical industries are discharged into the water every day. Presence of this dye in water causes considerable damage to the aquatic environment and human being coming in its contact. It is necessary to remove this compound from water. Several methods are used for this purpose it includes chemical precipitation and biological oxidation. Photocatalysis is one of the promising and effective methods used for degradation of organic compounds and dyes [1-3]. ZnO based semiconductors are widely used for this purpose. It has several advantages such as wide band gap (3.37 eV), nontoxicity, ease of crystallization, anisotropic growth, higher excitation binding energy (60 meV) and simplicity in tailoring the morphology [4-19]. However, due to its large band gap its uses are largely restricted to the ultraviolet (UV) light only,

which consists the 4 % of the total solar spectrum. To increase utility (in visible region) and enhance photocatalytic activity it is necessary to modify ZnO. This could be done by various ways such as doping it with metals or non-metals and coupling it with other semiconductors. Coupling of two semiconductors with different band gap energies is an effective approach to promote charge separation and minimize or inhibit charge-carrier recombination and to improve photocatalytic activity [20, 21]. They compensate the disadvantages of individual components and improve photo stability [22, 23]. Cadmium sulfide (CdS) is a very important II-VI semiconductor having band gap energy 2.42 eV and absorbs large amount of solar spectrum [24]. Recently, CdS nanoparticle based photocatalyst have been used to degrade dyes in presence of visible light [25, 26]. However CdS corrodes in aqueous environment. To overcome this stability problem CdS has been combined with wide band gap semiconductors like  $TiO_2$  and ZnO [27-29]. Lattice structure of CdS is similar to that of ZnO, which could build a close interaction between these two semiconductors. Thus, CdS is considered to be the most suitable visible light sensitizer for ZnO [30]. Recently many researchers have attempted to address the efficient development of heterojunctions of ZnO/CdS composite with different morphology [31-34]. Utilization of ZnO/CdS system alters optical and catalytic properties depending on the structure and morphology of the composite. In present work we report the microemulsion mediated synthesis of C/ZnO/CdS nanocomposite with enhanced photocatalytic activity. Structural, chemical and morphological details of

the photocatalysts have been studied. Optical properties of the nanocomposite have been investigated and finally the visible light photocatalytic activity of C/ZnO/CdS nanostructure for degradation of MB is studied.

## Experimental

### *Materials synthesis*

Methylene blue (MB) was procured from SD fine Chemicals Ltd. Mumbai and used without any further purification. Cyclohexane, n-butanol, N,N,N-cetyl trimethyl ammonium bromide (CTAB), acetone, cadmium nitrate ( $\text{Cd}(\text{NO}_3)_2 \cdot 4\text{H}_2\text{O}$ ), zinc nitrate ( $(\text{Zn}(\text{NO}_3)_2 \cdot 6\text{H}_2\text{O})$ ), sodium sulphide flakes ( $\text{Na}_2\text{S}$ ) (iron free), sodium hydroxide (NaOH) and ethanol (99.7%) all these chemicals used are AR grade and procured from SD Fine Chemicals Ltd. Mumbai and used without further purification.

### *Preparation of C/ZnO/CdS nanocomposite*

14.4 mL zinc nitrate, 2.95 g CTAB, 4 mL n-butanol and 17.6 mL cyclohexane were added in a beaker and solution was stirred for 30 min. To this solution, 14.4 mL 1M cadmium nitrate was added slowly with constant stirring. In another beaker 14.4 mL 2 M sodium hydroxide, 2.95 g CTAB, 4mL n-butanol, 17.6 mL cyclohexane and 14.4 mL 1M sodium sulphide was taken and mixture was stirred for 30 min. Both these solutions were mixed to each other with constant stirring. The resultant mixture was transferred to 250 mL Teflon-lined stainless steel autoclave and heated in an oven at 150 °C for 1h. After, the mixture was cooled and the residue formed was separated by centrifugation, washed with distilled water followed by ethanol and finally with acetone, then dried in an oven at 40 °C. Product thus formed was used as a precursor. The precursor was calcined in air at 300 °C for 2h to get C/ZnO/CdS nanocomposite. Pure and C doped ZnO was prepared using the microemulsion method reported in our previous work [35].

### *Preparation of nanosized CdS*

50mL 1M cadmium nitrate, 25 mL distilled water, 25mL ethanol and 0.01M CTAB were mixed in a beaker. To this solution 50mL 1M  $\text{Na}_2\text{S}$ , 25 mL ethanol and 25mL distilled water was added with vigorous stirring. To this mixture 20mL 2M NaOH was added with vigorous stirring to form light yellow precipitate. This mixture was transferred to Teflon-lined stainless steel autoclave and heated in an oven at 100 °C for 2h. After, it was cooled to the room temperature and the residue obtained was separated by centrifugation, washed several times with distilled water, ethanol and finally with acetone, then dried in oven at 40 °C, to get final product.

### *Characterization*

Thermal stability of C/ZnO/CdS precursor was studied using TG and DTA techniques (Rigaku, Model-Thermo plus TG8120). For recording TG and DTA curves 8.20mg of precursor was heated in flowing nitrogen atmosphere with a heating rate  $10^\circ\text{Cmin}^{-1}$ . For recording DTA curve, alumina was used as a reference material. XRD study of the

compounds synthesized in present work was carried out with X-ray diffractometer (XRD; Miniflex-II, Rigaku) using monochromatised Cu K( $\alpha$ ) radiation ( $\lambda = 1.54178 \text{ \AA}$ ) with a scan rate  $2^\circ\text{min}^{-1}$ . FTIR study of the compounds synthesized was carried out using Brooker FTIR spectrophotometer. Morphology and structure of the samples were examined using field emission scanning electron microscope (FE-SEM) (ZEISS; model Ultra-55). Compositional analysis was carried out using energy dispersive X-ray spectroscopy (EDX). The particle size of synthesized compounds was studied using a transmission electron microscope (Philips CM200). For the TEM analysis, the powders were dispersed in isopropyl alcohol and solution was sonicated for 15min. Few drops of the solution were loaded on a carbon coated copper grid and grid was dried under IR lamp for 30min. Optical absorption spectra of powder samples were recorded using a Shimadzu spectrophotometer (Model 1800) in the wavelength range of 200–850 nm. Photoluminescence spectra of samples were recorded at room temperature using Fluorescence spectrophotometer (Perkin Elmer-LS-55) with an excitation wavelength of 325 nm.

### *Photocatalytic activity study*

Reaction suspension was prepared by adding 0.05 g photocatalyst in 50mL (10ppm) MB solution. This aqueous suspension was stirred in the dark for 30min to attain adsorption-desorption equilibrium. Later the solution was irradiated with visible light. The visible light irradiation was carried out in a photo reactor using a compact fluorescent lamp (65 W,  $\lambda > 420 \text{ nm}$ , Philips, Mumbai). The distance between the fluorescent lamp and the reaction vessel was fixed at 10cm. Temperature of test solution was maintained constant throughout the experiment by circulating water around the solution. The reactant solution was irradiated under visible light for different time intervals. The catalyst was separated by centrifugation and the amount of MB in the supernatant solution was estimated from UV-visible spectrum recorded in the wavelength range 200-800 nm.

## Results and discussion

### *TG and DTA study*

TG and DTA curves of C/ZnO/CdS precursor were recorded and are presented in **Fig. 1(a)**. TG curve indicates that the mass of precursor decreases slowly up to 180 °C. It shows sudden decrease in mass in temperature range 200 to 300 °C. In temperature range 300 to 500 °C mass of precursor decreases steadily and above 570 °C there is no mass loss. DTA curve show small endothermic peak near 170 °C which is due to loss of free adsorbed water. The small exothermic peak near 250 °C is due to decomposition of the surfactant and residual OH group.

### *FTIR study*

FTIR spectra of C doped ZnO, pure CdS and C/ZnO/CdS are shown in **Fig. 1(b)**. All samples shows bands at 3411 and  $1628 \text{ cm}^{-1}$  attributed to stretching and bending modes of -OH group of water molecules adsorbed on the surface of

catalyst [36]. Band at  $2920\text{ cm}^{-1}$  and  $1114\text{ cm}^{-1}$  attributed to asymmetrical stretching of  $-\text{CH}_2$  group and symmetrical stretching of  $\text{C}-\text{OH}$  due to surfactant molecule. C doped ZnO and C/ZnO/CdS shows a band corresponding to Zn-O vibration near  $404\text{ cm}^{-1}$  [37, 38]. Pure CdS show a band at  $608\text{ cm}^{-1}$  ascribed to Cd-S stretching [39].

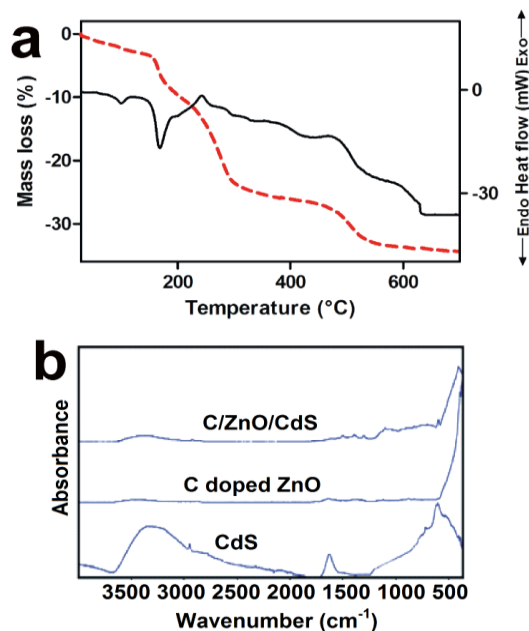


**Fig. 1** (a) TG and DTA curves of ZnO/CdS precursor in nitrogen atmosphere and (b) FTIR spectra of CdS, C doped ZnO and C/ZnO/CdS.

#### XRD study

XRD patterns of CdS, C doped ZnO and C/ZnO/CdS nanocomposites were recorded and are presented in **Fig. 2(a)**. XRD pattern of CdS shows peaks at  $2\theta$  equal to  $26.89$ ,  $44.12$  and  $52.19^\circ$  which corresponds to (111), (220) and (311) crystal planes of face centered cubic (FCC) CdS (JCPDS card no. 75-0581). Broadness of these peaks indicates that particles of CdS formed are very small. XRD pattern for C doped ZnO prepared at  $300^\circ\text{C}$  shows peaks at  $31.80$ ,  $34.44$ ,  $36.28$ ,  $47.46$ ,  $56.65$ ,  $62.86$ ,  $66.46$ ,  $67.98$ ,  $69.04$ ,  $72.64$  and  $77.0^\circ$  corresponds to (100), (002), (101), (102), (110), (103), (200), (112), (201), (004) and (202) crystal planes of ZnO respectively. It indicates that ZnO sample has a hexagonal wurtzite structure (JCPDS card no. 36-1451). XRD pattern of C/ZnO/CdS nanocomposite indicates the presence of FCC phase of CdS along with wurtzite ZnO phase. No other impurity phases are present. It also shows that intensity of ZnO peaks decreases with CdS coupling. Average crystalline size of CdS and ZnO nanoparticles were calculated using Debye-Scherrer equation and are found to be  $7.8$  and  $22.10\text{ nm}$  respectively. Crystallite size and lattice strain induced due to broadening is determined using Williamson-Hall (W-H) equation [40].

$$\frac{\beta \cos \theta}{\lambda} = \frac{1}{D} + \frac{4 \varepsilon \sin \theta}{\lambda}$$

where,  $\beta$  is the full width at half maximum (FWHM),  $\theta$  is diffraction angle,  $\lambda$  is X-ray wavelength,  $D$  is crystallite size and  $\varepsilon$  is lattice strain. Peak shift to lower angles in the

C/ZnO/CdS (**Fig. 2(a)** inset) is due to a smaller lattice constant for C/ZnO/CdS compared with pure and C doped ZnO. Plots of  $\beta \cos \theta / \lambda$  against  $4 \sin \theta / \lambda$  for pure as well as C doped ZnO and C/ZnO/CdS nanocomposite were plotted and are presented in **Fig. S1** (supplementary data). Slopes of these plots are  $+0.00078$ ,  $-0.0028$ ,  $-0.0013$ . Positive slope value for pure ZnO indicates the tensile strain and the crystallite size is  $34\text{ nm}$  (from intercept). Negative slope for C doped ZnO and C/ZnO/CdS composite indicates the presence of compressive strain and the crystallite size is  $25.1$  and  $21.8\text{ nm}$  respectively. These results reveals that tensile strain exists in pure ZnO nanorods, whereas C doped ZnO and C/ZnO/CdS nanocomposite have a compressive strain. This may be due to surface coating by CdS increases the compressive strain and leads to smaller crystallite size.

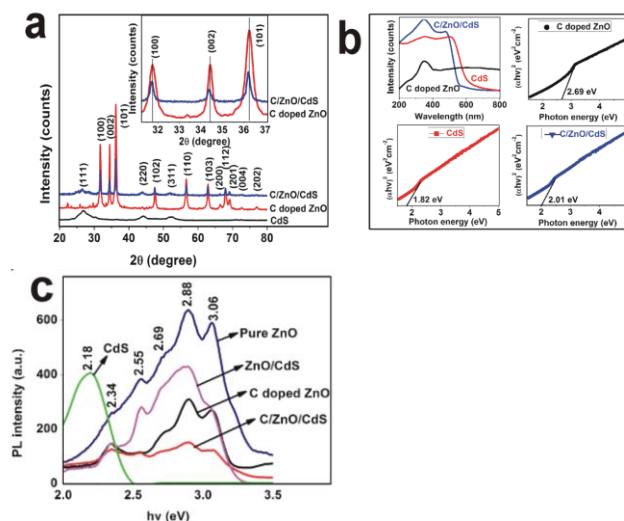


**Fig. 2** (a) XRD patterns of CdS, C doped ZnO and C/ZnO/CdS and inset shows expanded view, (b) UV-visible spectra and Tauc plots of C doped ZnO, CdS and C/ZnO/CdS nanocomposite and (c) Photoluminescence spectra of pure ZnO, CdS, ZnO/CdS, C doped ZnO and C/ZnO/CdS nanocomposite.

**Table 1.** Details of carbon content, lattice strain, crystallite size, band gaps and photocatalytic reaction parameters for samples.

Photocatalyst	Crystallite size (nm)	Carbon content (wt %)	Lattice strain	Band gap (eV)	Reaction parameters Rate constant (K min <sup>-1</sup> )	R <sup>2</sup>
CdS	7.8	-	-	1.82	0.00423	0.897
C doped ZnO	25.1	3.87	-0.0028	2.69	0.0369	0.924
C/ZnO/CdS	21.8	3.51	-0.0013	2.01	0.0732	0.914

EDX spectra of the synthesized compounds were recorded. From these spectra amount of C present in the samples was estimated and data obtained is presented in **Table 1**. It shows that amount of C present in ZnO and ZnO/CdS composite is  $3.87$  and  $3.51\%$ , respectively (by weight).

#### UV-visible absorption study

Band gap of C doped ZnO, CdS, and C/ZnO/CdS nanocomposite were estimated using Tauc plots from their UV-visible spectra (**Fig. 2(b)**). Black grey colour C doped ZnO sample gives absorption edge at  $460\text{ nm}$ , corresponding to band gap  $2.69\text{ eV}$ . This indicate that C-doped ZnO exhibit a red shift which results in a significant

enhancement of absorption in visible region. Pale yellow colour CdS nanoparticles exhibit band edge at 680 nm (1.82 eV), which is consistent with the band gap of cubic CdS. Band edge for C/ZnO/CdS is observed at 616nm (2.01eV), which indicates the ability of this nanocomposite to harvest the visible light. These result shows that CdS loading could help to increases the photoabsorption capacity of C doped ZnO in visible region.

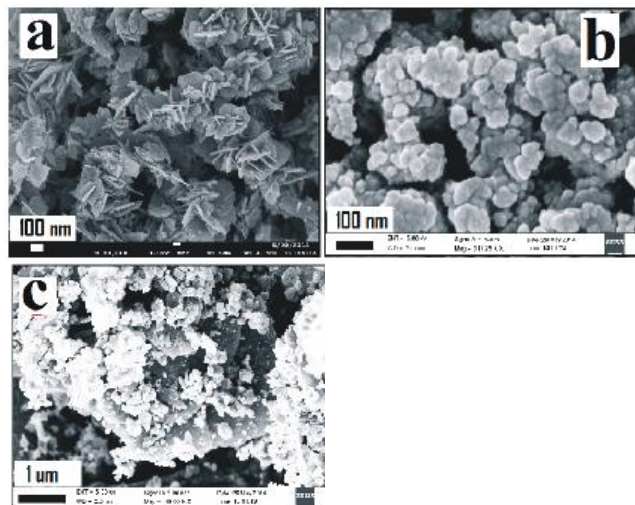


**Fig. 3.** FESEM images of (a) C doped ZnO, (b) CdS and (c) C/ZnO/CdS nanocomposite.

#### Photoluminescence study

Photoluminescence spectra of pure ZnO, CdS, ZnO/CdS, C doped ZnO and C/ZnO/CdS nanocomposite samples are shown in **Fig. 2(c)**. Pure ZnO has emission peaks at 3.06, 2.88, 2.69 and 2.56 eV. Emission centered at 3.06 eV is attributed to excitonic recombination corresponding to the near band edge emission of ZnO. The emission in the blue region at about 2.88 eV is associated with the electronic transition between excitonic level and interstitial oxygen (Oi). The emission in the blue-green region at 2.69 eV is attributed to the electron transition between a shallow donor (Zni) and a deep acceptor. The emission band in the green region (2.56 eV) is attributed to stoichiometry related defects and these are generally attributed to zinc vacancies as well as interstitial zinc and structural defects [31]. It is interesting to note that CdS has strong emission peak between 2.48 and 2.0 eV which is ascribed to surface defects associated with the cadmium and sulphur vacancies [41]. It is reported that surface defects as well as shallow and deep trap states are responsible for the luminescence property of CdS. ZnO/CdS nanocomposite shows PL quenching (as compared to pure ZnO). Also, the PL emission (2.34 eV) is blue shifted by about 0.15 eV as compared to pure CdS nanoparticles (2.19 eV), which is the evidence for electron transfer from CdS to ZnO on excitation. It is also observed that PL intensity of C doped ZnO is much lower as compared to pure ZnO. It can be seen that C/ZnO/CdS nanocomposite gives lower intensity PL peak as compared to ZnO, C doped ZnO and ZnO/CdS composite, which attribute to its higher photocatalytic activity. In C/ZnO/CdS system photo induced electrons and holes can be effectively separated and hence excitonic PL

intensity goes down. Photoluminescence effect, which is result of direct radiative recombination, lowers the recombination of generated carriers and causes the decrease of light emission intensity. This process simultaneously increases the photocatalytic activity of the semiconductors.

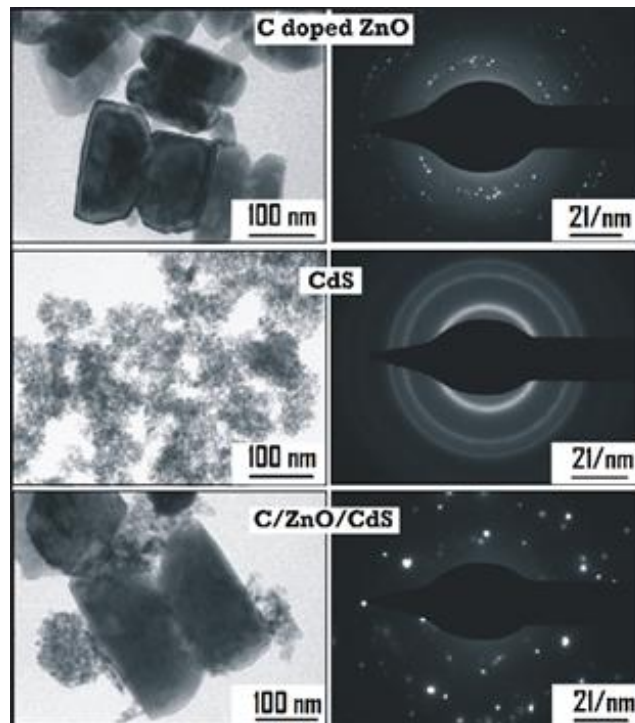


**Fig. 4.** TEM images and selected area electron diffraction patterns of C doped ZnO, CdS, and C/ZnO/CdS nanocomposite.

#### SEM study

FESEM images of CdS, C doped ZnO and C/ZnO/CdS nanocomposites are presented in **Fig. 3**. C doped ZnO prepared at 300°C is having irregular shape (**Fig. 3(a)**). It consist a mixture of rods and flakes. It also show (**Fig. 3(b)**) that CdS nanoparticles are nearly spherical in shape with particle size varies between ~6 to 10 nm. This image indicates that Cds particles are agglomerated. **Fig. 3(c)** shows that C/ZnO/CdS nanocomposite consists a mixture of flakes (C/ZnO), rods and spherical particles (CdS). It also shows that CdS particles are deposited on the surface of ZnO.

#### TEM study

TEM images of C doped ZnO, CdS and C/ZnO/CdS powders prepared in the present work are presented in **Fig. 4**. TEM image of C doped ZnO shows that these particles have a rod like structure. Average width and length of ZnO nanorods are 104 and 330nm respectively. TEM image of CdS nanoparticle confirms its spherical morphology with particle size varies between 8-10 nm. SAED pattern indicate the formation of well crystalline cubic CdS nanoparticles. TEM image of C/ZnO/CdS composite shows that CdS nanospheres were deposited on the surface of C doped ZnO nanorods. Selected area electron diffraction patterns (SAED) of the sample shows distinct rings that corresponds to the diffraction pattern of ZnO-CdS composite indicating crystalline nature.

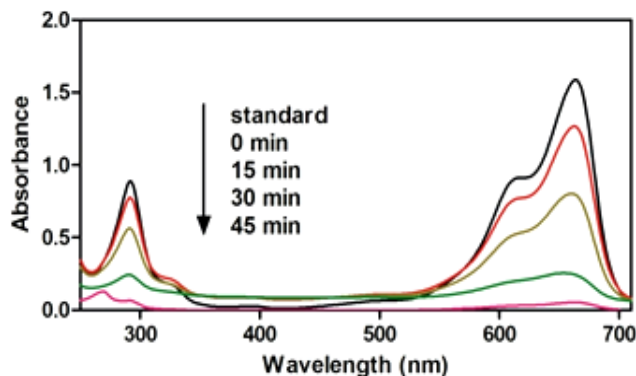


Fig. 5. UV-visible spectra of MB solution irradiated with visible light at different time intervals in presence of C/ZnO/CdS photocatalyst.

#### Photocatalytic activity study

UV visible spectra of aqueous solution of MB in presence of C/ZnO/CdS nanocomposite irradiated with visible light at different time intervals were recorded and are presented in Fig. 5. This spectrum shows characteristic peak maxima at 688 nm. In absence of catalyst there is no observable change in peak intensity which indicates that MB is stable in visible light. In presence of catalyst, peak maxima located at 688 nm decreases with increase in irradiation time. This may be due to photocatalytic degradation of MB. From UV-Visible spectra concentrations of MB remained in the solution at different time intervals were calculated. Similarly UV-visible spectra of MB in presence of different photocatalyst like pure and C doped ZnO, CdS were recorded.

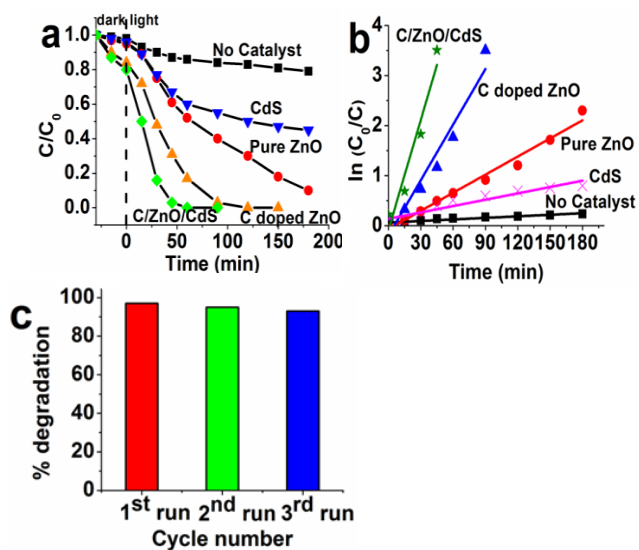


Fig. 6(a) Visible light photocatalytic degradation of MB In absence of catalyst, In presence of Pure ZnO, CdS, C doped ZnO and C/ZnO/CdS nanocomposite (b) Plot of  $\ln(C_0/C)$  versus irradiation time In absence of catalyst. In presence of Pure ZnO, CdS, C doped ZnO and C/ZnO/CdS nanocomposite (c) Cyclic runs showing photocatalytic degradation of MB in presence of C/ZnO/CdS nanocomposite.

Concentration of MB as a function of irradiation time in presence of photocatalyst was evaluated from its UV-visible spectra and data obtained is presented in Fig. 6(a). It is observed that as compared to pure ZnO, C doped ZnO shows higher adsorption efficiency for MB dye in dark this

may be due to the enhancement in the adsorption of organic pollutant assisted by doped C. In presence of C/ZnO/CdS core-shell nanocomposite ~98 % MB is degraded in 45min. This figure shows that nanocomposite exhibits better photocatalytic activity as compared to other photocatalysts. Enhanced photocatalytic activity of C/ZnO/CdS is due to effective loading of CdS on C doped ZnO nanorods which increases its photoabsorption capacity in visible region. Kinetics of MB degradation in visible light was studied. Graph of  $\ln(C_0/C)$  against irradiation time shows linear relationship, which indicate that photodegradation of MB follows first-order kinetics. The rate constants of MB degradation in presence of pure ZnO, CdS, C doped ZnO and C/ZnO/CdS photocatalyst are 0.0121, 0.00423, 0.0369, and 0.0732  $\text{min}^{-1}$  respectively (Fig. 6(b) and Table 1). The order of rate constants is C/ZnO/CdS > C doped ZnO > Pure ZnO > CdS. It is in good agreement with the results obtained for photocatalytic degradation curves presented in Fig. 6(a). The stability of catalyst was investigated by repeating the photodegradation process three times using the recovered photocatalyst and data obtained is presented in Fig. 6(c). This figure shows that up to third run there is no decrease in photocatalytic efficiency of catalyst and it is quiet stable.

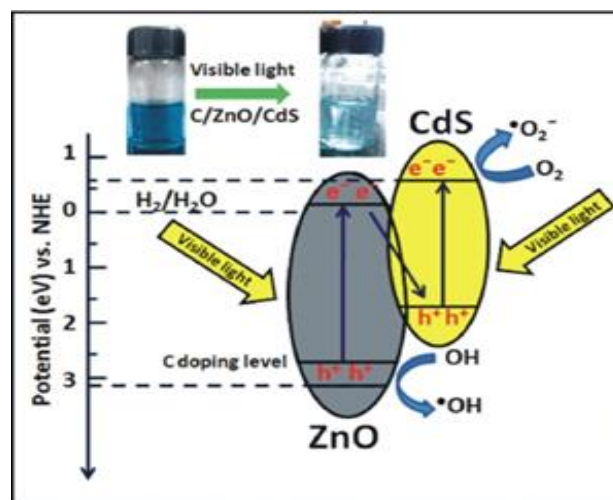


Fig. 7. Proposed band alignment of C/ZnO/CdS heterostructure and Z-scheme mechanism for visible light photocatalytic process.

#### Degradation mechanism

In photocatalysis, when semiconductor interacts with light of sufficient energy it produces reactive oxidizing species (ROS) which in turn give rise to photocatalytic conversion of organic pollutants. In photocatalysis process reactive oxidizing species produced via two simultaneous reactions. In first reaction photogenerated holes oxidize, dissociative adsorbed  $\text{H}_2\text{O}$  and in second reaction reduction of electron acceptor takes place by photo excited electrons. These two simultaneous reactions produce hydroxyl and superoxide radical anion respectively [42]. MB decomposes after reacting with  $\text{OH}^\bullet$  and  $\text{O}_2^\bullet$  reactive ions. The possible Z-scheme mechanism is presented in Fig. 7. C doping can effectively decreases the band gap of ZnO by forming energy level just above the valence band of ZnO. When C/ZnO/CdS nanocomposite is illuminated with visible light the photoexcited electron present in higher conduction band

minimum (CBM) of CdS transfers to the lower CBM of ZnO. Few photoexcited electrons in ZnO semiconductor with a lower CBM could combine with holes in the higher VBM of CdS. More powerful excited electrons and holes could be retained on both counterparts, which are responsible for formation of highly reactive superoxide radical anion ( $O_2^{\bullet-}$ ) and hydroxyl radicals ( $OH^{\bullet}$ ). These highly oxidative species decompose MB into  $H_2O$  and  $CO_2$ .

## Conclusion

In summary, C/ZnO/CdS nanocomposites were prepared using microemulsion method. XRD study indicates that the C/ZnO/CdS nanocomposite formed is the mixture consisting of ZnO (wurtzite) and CdS (cubic). From TEM and SEM results it is concluded that CdS nanospheres with particle size ~8 to 10 nm were grown on ZnO nanorods. Coupling of two semiconductors enhanced the visible light photo absorption capacity. C/ZnO/CdS nanocomposite shows lowest excitonic PL intensity, which increases the separation rate of photoinduced electrons and holes. As a result C/ZnO/CdS nanocomposite prepared in this work exhibits better visible light photocatalytic activity, compared to pure as well as C doped ZnO and CdS. The rate constant of MB degradation in presence of C/ZnO/CdS is  $0.0732 \text{ min}^{-1}$ , which is almost 6 times higher as compared to pure ZnO ( $0.0121 \text{ min}^{-1}$ ). The order of rate constants for photocatalytic degradation process using various photocatalyst is C/ZnO/CdS > C doped ZnO > Pure ZnO > CdS. Reusability study indicates that C/ZnO/CdS nanocomposite prepared in this work is highly stable and reusable photocatalyst.

## Acknowledgements

Authors are thankful to UGC, New Delhi for providing financial support. Authors are grateful to Sophisticated Analytical Instrumental Facility (SAIF), IIT, Mumbai for providing SEM and TEM facility.

## Author Contributions

AB - Performed the experiments, YS - Data analysis, Wrote the paper. It is declared that Authors have no competing financial interests.

## Reference

- Pawar, R C.; Lee, C S., *Appl. Catal. B.*, **2013**, *144*, 57.  
DOI: [10.1016/j.apcatb.2013.06.022](https://doi.org/10.1016/j.apcatb.2013.06.022)
- Lavand, A B.; Malghe, Y S., *Adv. Mater. Lett.*, **2015**, *6*, 695.  
DOI: [10.5185/amlett.2015.5800](https://doi.org/10.5185/amlett.2015.5800)
- Rahman, Q I.; Ahmad, M.; Misra, S K.; Lohani, M B., *Superlattices Microstruct.*, **2013**, *64*, 495.  
DOI: [10.1016/j.spmi.2013.10.011](https://doi.org/10.1016/j.spmi.2013.10.011)
- Becker, J.; Raghupathi, K R.; Pierre, J.; Zhao, D.; Koodali, R T. *J. Phys. Chem. C* **2011**, *115*, 3844.  
DOI: [10.1021/jp2038653](https://doi.org/10.1021/jp2038653)
- Bassaid, S.; Ziane, B.; Badaoui, M.; Chaib, M.; Robert, D., *Appl. Nanosci.*, **2013**, *3*, 211.  
DOI: [10.1007/s13204-012-0108-6](https://doi.org/10.1007/s13204-012-0108-6)
- Behera, D.; Acharya, B. S., *J. Lumin.*, **2008**, *128*, 1577.  
DOI: [10.1016/j.jlumin.2008.03.006](https://doi.org/10.1016/j.jlumin.2008.03.006)
- Macias-Sanchez, J J.; Hinojosa-Reyes, L.; Caballero-Quintero, A.; Cruz, W.; Ruiz-Ruiz, E.; Hernandez-Ramirez, A.; Guzman-Mar, L., *Photochem. Photobiol. Sci.*, **2015**, *14*, 536.  
DOI: [10.1039/c4pp00273c](https://doi.org/10.1039/c4pp00273c)
- Wu, C.; Zhang, Y C.; Huang, Q., *Mater. Lett.*, **2014**, *119*, 104.  
DOI: [10.1016/j.matlet.2013.12.111](https://doi.org/10.1016/j.matlet.2013.12.111)
- Panda, N R.; Acharya, B. S., *Mater. Res. Express*, **2015**, *2*, 015011.  
DOI: [10.1088/2053-1591/2/1/015011](https://doi.org/10.1088/2053-1591/2/1/015011)
- Bandekar, G.; Rajurkar, N S.; Mulla, I S.; Mulik, U P.; Amalnerkar, P V.; Adhyapak, P. V., *Appl. Nanosci.*, **2014**, *4*, 199.  
DOI: [10.1007/s13204-012-0189-2](https://doi.org/10.1007/s13204-012-0189-2)
- Nosrati, R.; Olad, A.; Maramfar, R., *Environ. Sci. Pollut. Res.*, **2012**, *19*, 2291.  
DOI: [10.1007/s11356-011-0736-5](https://doi.org/10.1007/s11356-011-0736-5)
- Srivastava, A K.; Deepa, M.; Bahadur, N.; Goyat, M S., *Mater. Chem. Phys.*, **2009**, *114*, 194.  
DOI: [10.1016/j.matchemphys.2008.09.005](https://doi.org/10.1016/j.matchemphys.2008.09.005)
- Lavand, A B.; Malghe, Y. S., *J. Asian Cer. Soc.*, **2015**, *3*, 305.  
DOI: [10.1016/j.jascer.2015.06.002](https://doi.org/10.1016/j.jascer.2015.06.002)
- Verma, R.; Mantri, B.; Ramphal; Srivastava, A. K., *Adv. Mater. Lett.*, **2015**, *6*, 324.  
DOI: [10.5185/amlett.2015.5661](https://doi.org/10.5185/amlett.2015.5661)
- Kuriakose, S.; Satpati, B.; Mohapatra, S., *Adv. Mater. Lett.*, **2015**, *6*, 217.  
DOI: [10.5185/amlett.2015.5693](https://doi.org/10.5185/amlett.2015.5693)
- Zeng, H.; Duan, G.; Li, Y.; Yang, S.; Xu, X.; Cai, W., *Adv. Fun. Mater.*, **2010**, *20*, 561.  
DOI: [10.1002/adfm.200901884](https://doi.org/10.1002/adfm.200901884)
- Gedamu, D.; Paulowicz, I.; Kaps, S.; Lupan, O.; Wille, S.; Haidarschin, G.; Mishra, Y K.; Adelung, R., *Adv. Mater.*, **2014**, *26*, 1541.  
DOI: [10.1002/adma.201304363](https://doi.org/10.1002/adma.201304363)
- Najim, M.; Modi, G.; Mishra, Y M.; Adelung, R.; Singh, D.; Agarwala, V., *Phys. Chem. Chem. Phys.*, **2015**, *17*, 22923.  
DOI: [10.1039/C5CP03488D](https://doi.org/10.1039/C5CP03488D)
- Wahab, R.; Ansari, S G.; Kim, Y S.; Seo, H K.; Kim, G S.; Khang, G.; Shin, H. S., *Mater. Res. Bull.*, **2007**, *42*, 1640.  
DOI: [10.1016/j.materresbull.2006.11.035](https://doi.org/10.1016/j.materresbull.2006.11.035)
- Meng, L.; Guoli F.; Lan, Yang.; Feng, Li., *RSC Adv.*, **2015**, *5*, 5725.  
DOI: [10.1039/C4RA07073A](https://doi.org/10.1039/C4RA07073A)
- Nayak, J.; Sahu, S N.; Kasuya, J.; Nozaki, S., *Appl. Surf. Sci.*, **2008**, *254*, 7215  
DOI: [10.1016/j.apsusc.2008.05.268](https://doi.org/10.1016/j.apsusc.2008.05.268)
- Kumar, A.; Jain, A. K., *J. Mol. Catal. A: Chem.*, **2001**, *165*, 265  
DOI: [10.1016/S1381-1169\(00\)00435-0](https://doi.org/10.1016/S1381-1169(00)00435-0)
- Qian, S.; Wang, C.; Liu, W.; Zhu, Y.; Yao, W.; Lu, X., *J. Mater. Chem.*, **2011**, *21*, 4945.  
DOI: [10.1039/C0JM03508D](https://doi.org/10.1039/C0JM03508D)
- Guerguerian, G.; Elhordoy, F.; Pereyra, C J.; Marotti, R. E.; Martin, F.; Leinen, D.; Ramos, B.; Jose, R.; Dalchiele, E A., *Nanotechnology*, **2011**, *22*, 505401.  
DOI: [10.1088/0957-4484/22/50/505401](https://doi.org/10.1088/0957-4484/22/50/505401)
- Shen, J.; Meng, Y.; Xin, G.; *Rare Metals*, **2011**, *30*, 280  
DOI: [10.1007/s12598-011-0285-6](https://doi.org/10.1007/s12598-011-0285-6)
- Shvalagin, V V.; Stroyuk, A L.; Kotenko, I E.; Kuchmii, S Y., *Theo. Exp. Chem.*, **2007**, *43*, 229.  
DOI: [10.1007/s11237-007-0026-y](https://doi.org/10.1007/s11237-007-0026-y)
- Jum, S J.; Hyun, G K.; Upendra, A J.; Ji, W J.; Jae, S. L., *Int. J. Hyd. Ene.*, **2008**, *33*, 5975.  
DOI: [10.1016/j.ijhydene.2008.07.105](https://doi.org/10.1016/j.ijhydene.2008.07.105)
- Guo, X.; Chen, C.; Song, W.; Wang, X.; Di, W.; Qin, W.; *J. Mol. Catal. A: Chem.*, **2014**, *1*, 387.  
DOI: [10.1016/j.molcata.2014.02.020](https://doi.org/10.1016/j.molcata.2014.02.020)
- Spanhel, L.; Weller, H.; Henglein, A., *J. Am. Chem. Soc.*, **1987**, *109*, 6632.  
DOI: [10.1021/ja00256a012](https://doi.org/10.1021/ja00256a012)
- Khanchandani, S.; Kundu, S.; Patra, A.; Ganguli, A K.; *J. Phys. Chem. C.*, **2012**, *116*, 23653.  
DOI: [10.1021/jp3083419](https://doi.org/10.1021/jp3083419)
- Kandula, S.; Jeevanandam, P., *J. Nanopart. Res.*, **2014**, *16*, 2452.  
DOI: [10.1007/s11051-014-2452-9](https://doi.org/10.1007/s11051-014-2452-9)
- Jana, T K.; Pal, A.; Chatterjee, K., *J. Alloys Comp.*, **2014**, *583*, 510.  
DOI: [10.1016/j.jallcom.2013.08.184](https://doi.org/10.1016/j.jallcom.2013.08.184)
- Geng, J.; Jia, X D.; Zhu, J. J., *Cryst Eng Comm.*, **2011**, *13*, 193.  
DOI: [10.1039/c0ce00180e](https://doi.org/10.1039/c0ce00180e)
- Li, C.; Ahmed, T.; Ma, M.; Edvinsson, T.; Zhu, J., *Appl. Catal. B: Environ.*, **2013**, *175*, 138.  
DOI: [10.1016/j.apcatb.2013.02.042](https://doi.org/10.1016/j.apcatb.2013.02.042)
- Lavand, A B.; Malghe, Y. S., *Int. J. Photocatal.*, **2015**, *1*, 790153.  
DOI: [10.1155/2015/790153](https://doi.org/10.1155/2015/790153)
- Wahab, R.; Kim, Y S.; Lee, K.; Shin, H S., *J. Mater. Sci.*, **2010**, *45*, 2967.  
DOI: [10.1007/s10853-010-4294-x](https://doi.org/10.1007/s10853-010-4294-x)

37. Bitenc, M.; Podbrscek, P.; Crnjak, O.Z.; Cleveland, MA.; Paramo, JA.; Peters, RM.; Strzhemechny, Y. M., *Cryst. Growth Des.*, **2009**, 9, 997.  
DOI: [10.1021/cg8008078](https://doi.org/10.1021/cg8008078)
38. Bitenc, M.; Crnjak, O. Z., *Mater. Res. Bull.*, **2009**, 44, 381.  
DOI: [10.1016/j.materresbull.2008.05.005](https://doi.org/10.1016/j.materresbull.2008.05.005)
39. Yang, G.; Yang, B.; Xiao, T.; Yan, Z., *Appl. Surf. Sci.*, **2013**, 283, 402.  
DOI: [10.1016/j.apsusc.2013.06.122](https://doi.org/10.1016/j.apsusc.2013.06.122)
40. Suryanarayana, C.; Norton, MG.; X-ray Diffraction: A practical Approach; *Plenum Publishing Corporation: New York*, **1998**.  
DOI: [10.1007/978-1-4899-0148-4](https://doi.org/10.1007/978-1-4899-0148-4)
41. Dhas, N A; Gedanken, A; *Appl. Phys. Lett.*, **1998**, 72, 2514.  
DOI: [10.1063/1.120624](https://doi.org/10.1063/1.120624)
42. Zhu, J.; Yang, D.; Geng, J.; Chen, D.; Jiang, Z., *J. Nanopart. Res.*, **2008**, 10, 729.  
DOI: [10.1007/s11051-007-9301-z](https://doi.org/10.1007/s11051-007-9301-z)

# Advanced Materials Letters

Copyright © 2016 VBRI Press AB, Sweden  
[www.vbripress.com/aml](http://www.vbripress.com/aml)

**Publish your article in this journal**

Advanced Materials Letters is an official international journal of International Association of Advanced Materials (IAAM, [www.iaamonline.org](http://www.iaamonline.org)) published monthly by VBRI Press AB from Sweden. The journal is intended to provide high-quality peer-review articles in the fascinating field of materials science and technology particularly in the area of structure, synthesis and processing, characterisation, advanced-state properties and applications of materials. All published articles are indexed in various databases and are available download for free. The manuscript management system is completely electronic and has fast and fair peer-review process. The journal includes review article, research article, notes, letter to editor and short communications.



**VBRI Press**  
a rapid publication platform

**A Monthly Journal**

February 2016

**Advanced Materials Letters**

ISSN 2151-1141

Available online at [www.vbripress.com](http://www.vbripress.com) and [www.iaamonline.org](http://www.iaamonline.org)

## Supporting Information

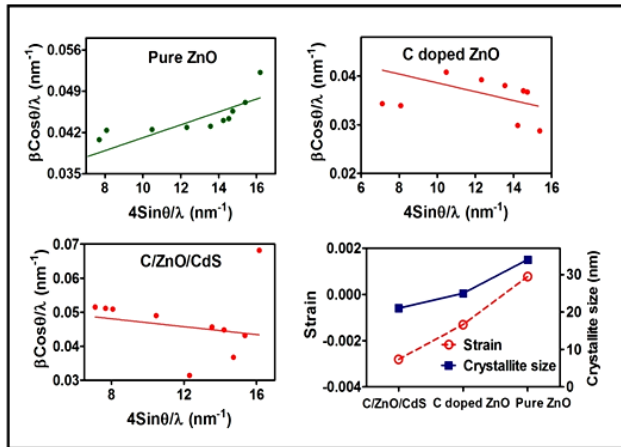


**Fig. S1.** Williamson-Hall (W-H) plot :  $\beta \cos \theta / \lambda$  versus  $4 \sin \theta / \lambda$  and relation between strain and crystallite size for pure ZnO, C doped ZnO and C/ZnO/CdS nanocomposite.